The International Journal of Advanced Manufacturing Technology (2018) 97:1733–1743
https://doi.org/10.1007/s00170-018-2051-5

ORIGINAL ARTICLE

Utilization of heat quantity to model thermal errors of machine tool spindle

Shuanggang Huang[1] · Pingfa Feng[1,2] · Chao Xu[1] · Yuan Ma[1] · Jian Ye[1] · Kai Zhou[1]

Received: 14 October 2017 / Accepted: 17 April 2018 / Published online: 1 May 2018

Abstract
Thermal error modeling of the spindle plays an important role in predicting thermal deformation and improving machining precision. Even though the modeling method using temperature as the input variable is widely applied, it is less effective due to severe loss of thermal information and pseudo-hysteresis between temperature and thermal deformation. This paper presents a novel modeling method considering heat quantity as the input variable with theoretical analysis and experimental validation. Firstly, the change of thermal state of a metal part being heated is discussed to reveal the essence of the relationship between heat, thermal deformation and temperature, and the theoretical basis of the modeling method proposed in this paper is elaborated. Subsequently, the relationship between thermal deformation and heat quantity is further studied through modeling the thermal deformations of stretching bar and bending beam using heat quantity as the independent variable, and the stretching model is verified based on finite element method. Then, the thermal error models of the spindle are developed with the heat elastic mechanics theory and the lumped heat capacity method. In succession, the parameter identification of thermal error models is carried out experimentally using the least square method. The average fitting accuracy of these models is up to 91.3%, which verifies the good accuracy and robustness of the models. In addition, these models are of good prediction capability. The proposed modeling method deepens the research of thermal errors and will help to promote the application of relevant research results in the actual production.

Keywords Thermal error · Spindle · Modeling · Heat quantity · Prediction

1 Introduction

With the development of modern mechanical industry, the demand of high precision of machine tools becomes higher and higher. Thermal error caused by the heating is one of the principal causes of the imprecision and accounts for 40–70% of the total error [1]. Therefore, study on thermal errors has become one of the research hotspots in the field of precision machining in recent years. Thermal error modeling is the key step of error compensation and also a technical difficulty due to the complexity of the mechanism causing the machine tool deformations [2].

The spindle system is a major component and the maximum heat source in machine tools [3], and its thermal deformation has a significant adverse effect on machining precision and thus is the focus of the present research on thermal problems of machine tools [4–6]. Most precision machine tools are equipped with high-speed motorized spindles [7, 8]. Unlike the conventional spindle systems, the high-speed motorized spindle generates a great deal of heat when the current flows into the built-in motor due to the copper loss, iron loss and windage power loss [9, 10]. Simultaneously, a large amount of heat is generated near the bearing's contacts due to the friction between the balls and the inner and outer races [11, 12]. In

Highlights Methodology of utilization of heat quantity in thermal error modeling was developed.
Method of modeling error by developing a system of typical models was proposed.
Thermal error model expressed as the function of heat quantity showed high accuracy.
Models predicted thermal error well and optimized the processing technology.

✉ Chao Xu
xu.chao@sz.tsinghua.edu.cn

[1] Division of Advanced Manufacturing, Graduate School at Shenzhen, Tsinghua University, Shenzhen 518055, People's Republic of China

[2] Department of Mechanical Engineering, Tsinghua University, Beijing 100084, People's Republic of China

addition, because of its complex structure, poor cooling conditions, and complex internal coupling relations [13], the thermal problems in high-speed motorized spindle are more severe [14–16]. Therefore it is urgent to study the thermal deformation of the spindle of precision machine tools.

The goal of studying thermal deformations is to develop thermal error models with good accuracy and robustness. Most scholars had attempted to develop thermal error models with temperature as their input [17–19]. When monitoring the temperature field of a machine tool, only a limited number of surface temperature readings can be measured simultaneously, which contributes to a severe loss of thermal information. Also, the selection of thermal key points is complicated and there are as yet no generally accepted methods for selecting the thermal key points [20]. Therefore, it is difficult to accurately characterize the thermal state of the machine tool with the measured temperature readings. Moreover, there is a pseudo-hysteresis between temperature and thermal deformation [21, 22], which makes the thermal error model with temperature as its input variable less precise and robust. Some scholars also tried to take multiple variables, such as the spindle speed, motor current and historical information etc., as the inputs to thermal error models [10, 23, 24]. However, few articles carried out a rigorous theoretical demonstration of the reasons for the adoption of relevant variables, and the experimental schemes presented in these articles were often too complex to implement. Therefore, the mechanism of thermal deformations should be further studied and a more scientific and efficient modeling method should be explored.

The thermal deformation is essentially a macroscopic behavior of thermoelastic distortion caused by the heat absorbed in the machine tool [25]. The degree of thermal deformation is closely related to the quantity of heat absorbed. Therefore, it is possible to characterize the thermal state of the machine tool using the heat quantity absorbed in it.

In addition, the thermo-mechanical properties of the spindle system are related to machine tool structures [5, 26]. So the machine tool structure needs to be studied before thermal error modeling. As the machine tool is made up of parts of various shapes, developing a complete system of thermal deformation models of typical parts of machine tools will be helpful to studying its thermal deformations. Then, based on the study of the structural characteristics of the machine tool, the thermal deformations of the spindle can be studied with a clearer direction and so more efficiently.

In this paper, the essence of the relationship between heat, thermal deformation, and temperature is discussed and the theoretical basis of the modeling method proposed is elaborated firstly. Subsequently, the relationship between thermal deformation and heat quantity is further studied through modeling the thermal deformations of stretching bar and bending beam using heat quantity as the independent variable. Then, the thermal error models of the spindle in the constant temperature workshop running at idle are developed and the parameter identification of these models is carried out experimentally. Finally, the main results of this paper are discussed and concluded.

2 Relationship between thermal deformation and heat quantity

2.1 Changes of thermal state during heating

As is known, the spindle will undergo temperature rise and thermal deformation due to the heat generated when the machine tool runs. In order to calculate the thermal deformation, a suitable thermal state equation should be sought. Most scholars had attempted to establish a state equation describing the relationship between temperature and thermal deformation.

However, the fact is that there is no direct correspondence between temperature and thermal deformation. Taking a metal part being heated as an example to illustrate this point, the temperature and thermal deformation of the metal part don't change synchronously. Especially when the part is heated to melt, its temperature will not change while its shape changes and undergoes volume increase, as shown in Fig. 1. In this case, rather than temperature, only the heat quantity absorbed in the part can be used to calculate the change of its volume.

According to the lattice vibration theory, the relationship between the expansion coefficient and the heat capacity of the metal body is derived by Eduard Grüneisen as follows [27]:

$$\beta = \frac{\gamma}{KV} C_v, \tag{1}$$

where β is the coefficient of volume expansion, γ is the Grüneisen parameter, K is the bulk modulus, V is the sample volume, and C_v is the heat capacity at constant volume. For the cubic system, the expansion coefficient is the same in all

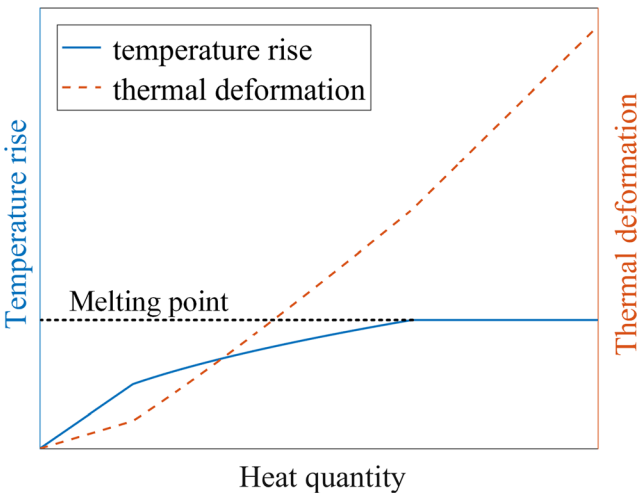

Fig. 1 Changes of thermal state when the metal part is heated

directions, $\beta = 3\alpha$ (α is the coefficient of linear expansion). Hence, the heat capacity is given as follows:

$$C_v = \frac{3KV\alpha}{\gamma}. \tag{2}$$

It is known from Eq. (2) that as for the isotropic material, the heat capacity changes synchronously with the expansion coefficient, and that is the thermal deformation of a part is closely related to the heat quantity absorbed. Therefore, a state equation describing the relationship between heat quantity and thermal deformation should be sought to model thermal errors of the machine tool spindle.

2.2 Methodology of utilization of heat quantity in thermal error modeling

The thermal deformation of a part is related to its shape and the locations of heat sources on it. As the machine tool is made up of parts of various shapes, developing a system of thermal deformation models of typical machine tool parts with heat quantity as the input will be very helpful to studying its thermal errors. In this section, two thermal deformation models are presented to help the analysis of spindle thermal error.

(1) Stretching model There are many long parts in machine tools such as the spindle and the linear guide, whose main thermal deformations are in the length direction. For such parts, the relationship between thermal deformation and heat quantity is analyzed with a member bar as the specimen. The length and the cross-sectional area of the specimen are L and S, respectively. The left end of the specimen is considered at the origin of the X axis and the specimen has an internal heat source to heat itself, as shown in Fig. 2.

It is well known that the thermal stretching of a member bar is proportional to its average temperature rise. However, the temperature changes (ΔT) in different axial positions on the specimen are various and not synchronized with the total thermal deformation (as shown in Fig. 3). It is difficult to accurately calculate the average temperature rise with the measured temperature readings. Also, the asynchronism between temperature changes and thermal deformation causes the poor accuracy and robustness of thermal error models using temperature as the input variable. It is obvious from the above that even for a specimen with regular shape and simple heating conditions, expressing its thermal deformation using temperature is much complex and difficult. Therefore, a new and more efficient modeling method should be explored. In the following sections, the thermal error modeling will be studied from the point of view of heat.

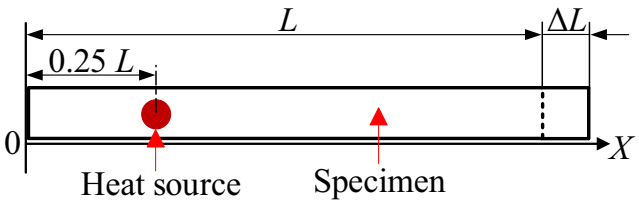

Fig. 2 Stretching model

Assuming the distribution function of temperature rise of the specimen in X direction is $T(x)$ (as shown in Fig. 4) and the linear expansion coefficient is α, the thermal deformation is given as follows:

$$\Delta L = \int_0^L \alpha T(x) dx. \tag{3}$$

Assuming that the specific heat capacity and the density of the specimen material are c and ρ, respectively, then the heat quantity absorbed in the specimen is

$$E = \rho \int_0^L cT(x) S dx. \tag{4}$$

According to Eqs. (3) and (4), the relationship between thermal deformation and heat quantity is given as follows:

$$\Delta L = \frac{\alpha E}{\rho c S}. \tag{5}$$

It can be seen from the above equation that the thermal stretching (ΔL) of the specimen is independent of the location of the heat source and the temperature distribution, and is proportional to the quantity of heat absorbed (E). This model is called the stretching model. Based on finite element method, temperature field and thermal deformation simulation of the specimen is implemented to verify Eq. (5). The parameters of the specimen are shown in Table 1.

Two groups of thermal simulation experiments are carried out to verify the stretching model. In Experiments 1 and 2, heat flow load is applied at one end and the middle of the specimen, respectively. The initial temperature of the specimen is 22 °C. Axial thermal deformations of the specimen in Experiments 1 and 2 and calculated with Eq. (5) are denoted by δ_1, δ_2, and δ_3, respectively. The nephograms of temperature

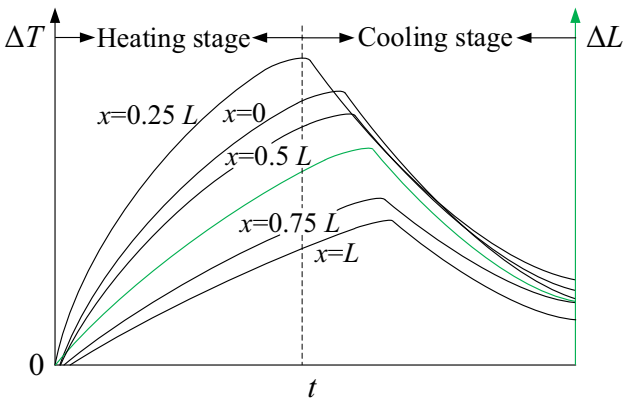

Fig. 3 Temperature changes in different axial positions

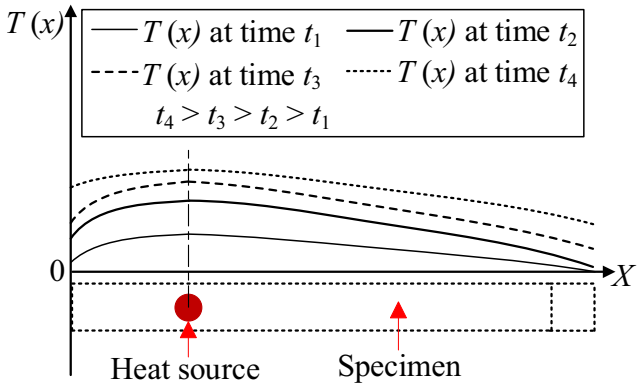

Fig. 4 Distribution function of temperature rise during heating stage

field of the specimen in both experiments with the same heat flow load are shown in Fig. 5. Axial thermal deformations with heat quantity as independent variable are shown in Table 2. It can be seen from Fig. 5 and Table 2 that even though the temperature distribution is different when the position of heat source is changed, there will be no difference in overall axial thermal deformations as long as the heat quantity absorbed is the same. The simulation results are in good agreement with the calculation results of Eq. (5) and the correctness of the stretching model is well verified.

It can be seen from Fig. 4 that the distribution function of temperature rise of a part is complex and time-varying and thus is difficult to derive. When the thermal deformations are investigated with the proposed stretching model, it can be assumed that the temperature field of the part distributes uniformly in space and the temperature gradient can be ignored. Therefore the part temperature is expressed by the average temperature, and this method is called the lumped heat capacity method. The average temperature of the part can easily be obtained by the quantity of heat absorbed. It is known from the above theoretical analysis that this model can ensure the accuracy of thermal deformation calculation and significantly reduce the complexity of the thermal issue.

Table 1 Specimen parameters

Parameter	Value	Unit
Length	1	m
Cross-sectional diameter	0.1	m
Material property	Value	Unit
ρ	7850	kg/m^3
α	1.13	10^{-5}/°C
E'	200	GPa
μ	0.3	
λ	50.66	W/(m.°C)
c	477	J/(kg.°C)

(2) Bending model Large machine tools such as guideway grinder, milling planer, and double housing planer, etc., they all have long beds. The temperature readings of the bed's upper surface are higher than that of the bottom surface due to cutting heat during processing, which makes the bed to bend into a convex shape. The thermal deformation of the bed can be analyzed with a bending model, as shown in Fig. 6. The bed length is L, bed height is H, and the thermal deformation of concern is ΔH.

According to the stretching model, ΔL is given as follows:

$$\Delta L = \frac{\alpha E}{\rho c S}, \tag{6}$$

$$\theta = \frac{\Delta L}{H}, \tag{7}$$

$$\Delta H = \frac{L}{2\sin\theta} - \frac{L\cos\theta}{2\sin\theta}. \tag{8}$$

According to Eqs. (6), (7), and (8), the relationship between thermal deformation and heat quantity is given as follows:

$$\Delta H = \frac{L}{2}\left(1-\cos\frac{\alpha E}{\rho c S H}\right)/\sin\frac{\alpha E}{\rho c S H}. \tag{9}$$

From Eq. (9), it can be seen that the thermal deformation of the specimen is a trigonometric function of heat quantity, and this model is called the bending model.

It is known from the above two thermal deformation models (i.e., stretching and bending models) that thermal deformations are functions of heat quantity. Therefore, it is feasible to develop thermal error models considering heat quantity as their input. Also, according to the thermal deformation characteristics of key parts of machine tools, more thermal deformation models can be developed to facilitate the analysis of thermal deformations of machine tools.

There are two key technologies in analyzing the thermal deformations of a machine tool using the proposed method, one is the calculation of heat quantity absorbed in the machine tool, and the other is the simplification of machine tool structure, as shown in Fig. 7. The advantage of this method lies in that the accuracy of thermal error models can easily be improved through improving the calculation accuracy of heat quantity and reducing the simplification degree of machine tool structure to meet the required machining precision.

2.3 Thermal deformation calculation using heat quantity

The machine tool studied in this paper is equipped with a high-speed motorized spindle. Before analyzing the machine tool's thermo-mechanical properties, it is necessary to identify its structural characteristics and simplify its structure appropriately. The machine tool structure has the following features:

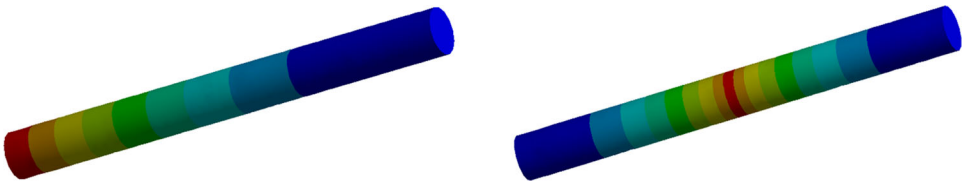

(a) Nephogram of temperature field when left end being heated

(b) Nephogram of temperature field when the middle being heated

Fig. 5 Nephograms of temperature field (heat flow is 10 W and heating time is 20 h)

(1) The dimension of the spindle system in Z direction is much larger than that in X and Y directions.

(2) The dimension of the spindle system is much smaller than that of the beam in Y direction.

(3) The spindle system and the beam are symmetrical with respect to YZ plane.

A simplified model of the machine tool structure is presented considering its structural characteristics, as shown in Fig. 8. Although the structural simplification will reduce the calculation complexity of thermal deformations, it may lead to a decrease in calculation accuracy. The required machining precision dictates the extent to which simplification can be made.

When the spindle runs at high speed, the spindle system will generate a large amount of heat inside due to mechanical losses and electromagnetic losses. The heat is conducted to the surroundings in all directions, which mainly results in thermal deformations of both the spindle system and the beam. This further results in a thermal displacement of the tool center point (TCP) relative to the machine table.

The thermal displacement of the TCP relative to the machine table consists of the thermal displacement of the TCP and the thermal deformation of the table. As the spindle and the beam are both long parts and the concerned thermal deformations of them are along the length direction, the stretching model is suitable for calculating the thermal displacement of the TCP. While machining workpieces, a great deal of cutting heat is transferred to the upper surface of the machine table, which makes the temperature readings of the upper surface are higher than that of the lower surface. Therefore, the thermal deformation of the table can be calculated using the bending model.

When the spindle in the constant temperature workshop runs at idle, the machine table will not undergo any thermal deformation. Hence, the thermal displacement of the TCP relative to the machine table is caused only by the thermal deformations of the spindle system and the beam.

Table 2 Axial thermal deformations when heated

Heat absorbed (kJ)	δ_1 (μm)	δ_2 (μm)	δ_3 (μm)
180	69.60	69.75	69.17
360	139.39	139.61	138.33
540	209.22	209.47	207.51
720	279.06	279.33	276.68

There are two main heat sources when the spindle runs, one comes from the copper and iron losses when the current flows into the built-in motor (heat generation power is denoted by q_1), the other is due to the friction between the bearing's contacts (heat generation power is denoted by q_2). When the spindle speed remains constant, q_1 is a constant. q_2 is calculated by the following equation [28]:

$$q_2 = 1.047 \times 10^{-4} nM, \tag{10}$$

where n is the rotating speed, M is the total frictional torque of the bearing. As n and M are constants, so q_2 remains constant, too.

It can be assumed from the above analysis that there is a constant-power heat source inside the spindle when the spindle speed does not change. The average surface temperature ($\overline{T}$) of the spindle system is given as follows:

$$\overline{T} = \int_0^S \frac{T_\sigma}{S} d\sigma, \tag{11}$$

where T_σ is the average temperature of local area σ and S denotes the total surface area of the spindle system. The heat dissipation power to the air (q_{out}) is given as follows:

$$q_{out} = K^{'}\left(\overline{T} - T_0\right) S, \tag{12}$$

where K' is the surface heat transfer coefficient and T_0 is the ambient temperature. At time t, the heat quantity absorbed in the spindle system (Q_{in1}) is

$$Q_{in1} = \int_0^t (q_{all} - q_{in2} - q_{out}) dt, \tag{13}$$

where q_{all} and q_{in2} denote the heat generation power and heat transfer power from the spindle system to the beam, respectively.

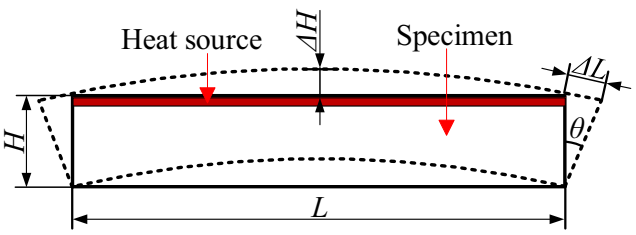

Fig. 6 Bending model

Q_{in1} can also be expressed as

$$Q_{in1} = C_1\left(\overline{T}-T_0\right) = a\overline{T} + b, \tag{14}$$

where a and b are constants and C_1 is the heat capacity of the spindle system. According to Eqs. (12), (13), and (14), the following result can be derived:

$$\overline{T} = de^{-t} + f, \tag{15}$$

where d and f are constants. The Z-directional thermal displacement of the TCP (δ_z) is

$$\delta_z = \alpha_1 L\Delta T_1 = \alpha_1 L\left(\frac{T_s+\overline{T}}{2}-T_0\right), \tag{16}$$

where α_1 is the linear expansion coefficient of the spindle, ΔT_1 is the average temperature rise of the spindle, and T_S is the temperature of where near the internal heat source of the spindle. T_S rises rapidly and enters a steady-state in so short a time that can be assumed as constant. Hence, Eq. (16) can be rewritten as

$$\delta_z = g\overline{T} + h, \tag{17}$$

where g and h are constants. According to Eqs. (15) and (17), the above equation can be simplified to

$$\delta_z = ie^{-t} + j, \tag{18}$$

where i and j are constants. It can be seen from Eq. (18) that the Z-directional thermal displacement of the TCP is an exponential function of time.

The Y-directional thermal displacement of the TCP (δ_y) is

$$\delta_y = \alpha_2 L_2\Delta T_2 + \alpha_1 L_1\Delta T_1, \tag{19}$$

where α_2 is the linear expansion coefficient of the beam and ΔT_2 is the average temperature rise of the beam. The heat quantity absorbed in the beam (Q_{in2}) is given as follows:

$$Q_{in2} = \rho c_2 V_2\Delta T_2 = \rho c_2 S_2 L_2\Delta T_2, \tag{20}$$

where c_2 is the specific heat capacity of the beam, V_2 is the volume of the beam and S_2 is the cross-sectional area of the beam along Y direction. Therefore, Eq. (19) can be further simplified as follows:

$$\delta_y = \frac{\alpha_2 Q_{in2}}{\rho c_2 S_2} + \alpha_1 L_1\Delta T_1 = \frac{\alpha_2 q_{in2} t}{\rho c_2 S_2} + \alpha_1 L_1\Delta T_1. \tag{21}$$

Due to the large heat capacity of the beam, q_{in2} can be assumed as constant for a long period of time. Thus, Eq. (21) can be rewritten as follows:

$$\delta_y = \frac{\alpha_2 q_{in2} t}{\rho c_2 S_2} + \alpha_1 L_1\Delta T_1. \tag{22}$$

Due to the dimension of the spindle system in Y direction is much small, and also for the spindle system will soon reach a thermal equilibrium state compared to the beam, the second term of the right-hand side of the above equation can be assumed as a constant and Eq. (22) can be written in a simplified equation as follows:

$$\delta_y = kt + l, \tag{23}$$

where k and l are constants. It can be seen from Eq. (23) that the Y-directional thermal displacement of the TCP is a linear function of time.

From the above analysis, the Z-directional and Y-directional thermal error models are obtained. The models will be experimentally verified in the following section. It should be noted that as the spindle system and the beam are symmetrical with respect to YZ plane, the X-directional thermal displacement of the TCP is so small that will not be discussed in this paper.

3 Model identification and thermal error prediction

3.1 Experimental setup

The established thermal error models were verified experimentally in this section. The experiments were carried out in a constant temperature workshop (21.4–21.8 °C) and the experimental setup is shown in Fig. 9. The experimental principle is shown in Fig. 10. Laser displacement Sensor 1 measures the Z-directional thermal displacement and Sensor 2 measures the Y-directional thermal displacement. Two groups of experiments were carried out. In Experiment 1, the spindle speed was set at 6000 rpm where as in Experiment 2, it was set at 8000 rpm. These two spindle speeds are widely used in industrial production. The experiments were conducted till the machine tool reaches a thermal equilibrium state.

3.2 Model parameter identification

3.2.1 Z-directional thermal error model identification

According to Eq. (18), there is a linear relationship between the Z-directional thermal displacement of the TCP (δ_z) and e^{-t}. When the spindle runs at 6000 rpm, the correlation coefficient between δ_z and e^{-t} is 0.9974. Therefore, the Z-directional thermal error has a good linear relationship with e^{-t}. Based on the least squares linear fitting algorithm, the Z-directional thermal error model is given as follows:

$$\delta_z = ie^{\frac{-t}{3400}} + j, \tag{24}$$

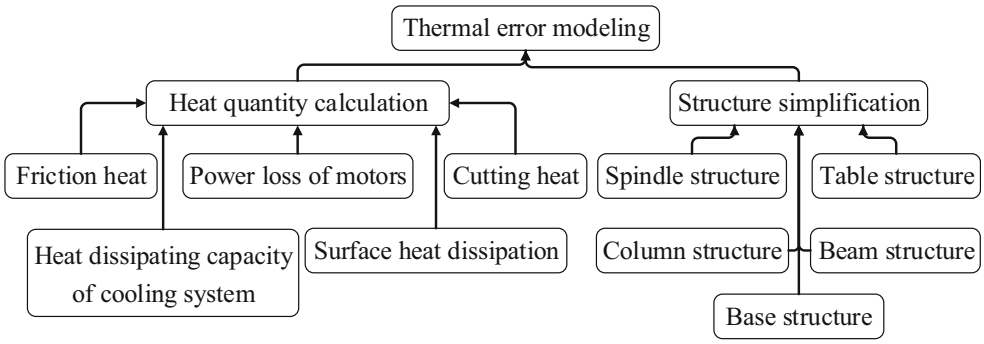

Fig. 7 Technology roadmap of thermal error modeling

where i is − 14.04 and j is 14.05. The fitting effect is shown in Fig. 11. The fitting residual is as small as 2.2%, which verifies the accuracy of the proposed model.

When the spindle runs at 8000 rpm, the correlation coefficient between δ_z and e^{-t} is 0.9851. The Z-directional thermal error model is given as follows:

$$\delta_z = ie^{\frac{-t}{3400}} + j, \tag{25}$$

where i is − 8.39 and j is 6.02. The fitting effect is shown in Fig. 12. The fitting residual is 21.8%, which shows that this model is of good accuracy. But on the other hand, the model is not well fitted with the experimental data in the first 3 min of the experiment, which is due to the slight oversimplification performed on the machine tool structure.

As can be seen from Figs. 11 and 12, the Z-directional thermal displacement has the characteristic of periodic fluctuation, and the fluctuation cycle at 8000 rpm is shorter than that at 6000 rpm. This is because the cooling system of the machine tool works periodically, and the working cycle is shortened as the spindle speed increases. In addition, the maximum thermal deformation at 8000 rpm is smaller than that at 6000 rpm for the cooling power increases as the speed rises.

The presented research results verify that the Z-directional thermal error model proposed is of high accuracy and good robustness.

3.2.2 Y-directional thermal error model identification

It is known from Eq. (23) that there is a linear relationship between the Y-directional thermal displacement of the TCP (δ_y) and time (t). When the spindle runs at 6000 rpm, the correlation coefficient between δ_y and t is 0.9966. Thus, the Y-directional thermal error has a good linear relationship with time. Based on the least squares linear fitting algorithm, the Y-directional thermal error model is given as follows:

$$\delta_y = k \times 10^{-4} t + l, \tag{26}$$

where k is − 5.44 and l is 0.29. The fitting effect is shown in Fig. 13. The fitting residual is only 4.7%, which validates the accuracy of the proposed model.

When the spindle runs at 8000 rpm, the correlation coefficient between δ_y and t is 0.9696. The Y-directional thermal error model is

$$\delta_y = k \times 10^{-4} t + l, \tag{27}$$

where k is − 3.87 and l is − 1.27. The fitting effect is shown in Fig. 14. The fitting residual is 6.0%, which confirms the accuracy of the proposed model.

It can be seen from Figs. 13 and 14 that just like the Z-directional thermal displacement, the Y-directional thermal displacement has the characteristic of periodic fluctuation, and the fluctuation cycle at 8000 rpm is shorter than that at 6000 rpm, which confirms that the cooling system of the machine works periodically, and the working cycle is shortened as the spindle speed increases. Also, the maximum thermal deformation at 8000 rpm is smaller than that at 6000 rpm, which confirms that the cooling power increases as the speed rises.

The above research results verify that the proposed Y-directional thermal error model is of high accuracy and good robustness. Moreover, it is obvious that the robustness of the proposed Y-directional thermal error model is superior to that of the Z-directional thermal error model. This is due to the over-simplification of the spindle structure which mainly

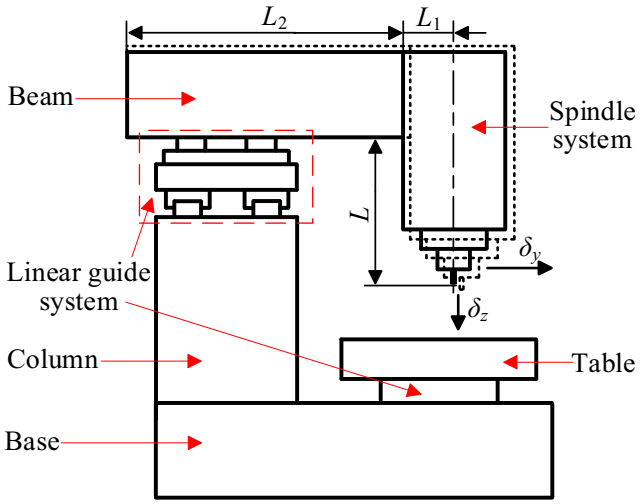

Fig. 8 Machine tool structure

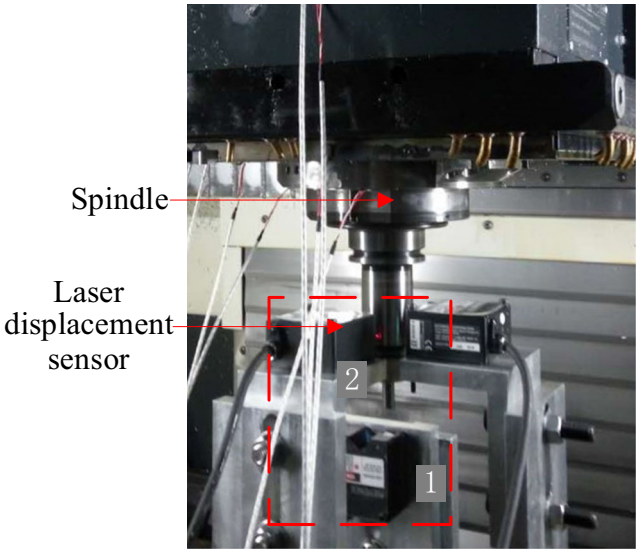

Fig. 9 Experimental setup

results in degraded calculation accuracy of the *Z*-directional thermal deformation.

3.3 Thermal error prediction

3.3.1 Z-directional thermal error prediction

According to Eqs. (24) and (25), the *Z*-directional thermal error prediction model is given as follows:

$$\delta_z = i(s)e^{\frac{-t}{\tau}} + j(s), \tag{28}$$

where s is the spindle speed, τ is the time constant of the machine tool which is independent of the spindle speed, $i(s)$ and $j(s)$ are functions of s whose absolute values decrease with the increase of the spindle speed. As far as the machine tool studied in this paper is concerned, the time constant is 3400 s.

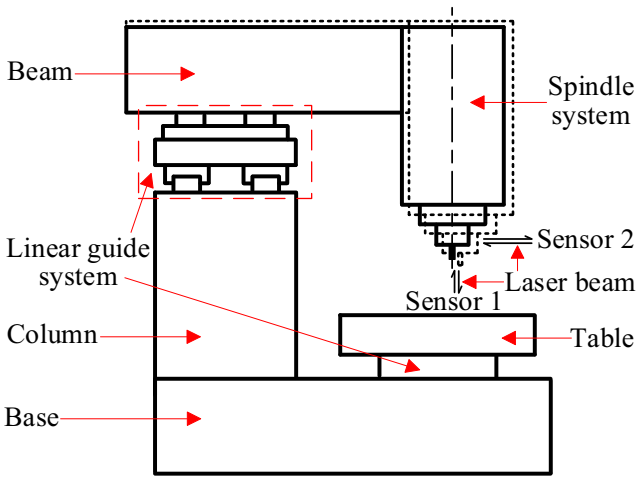

Fig. 10 Experimental principle

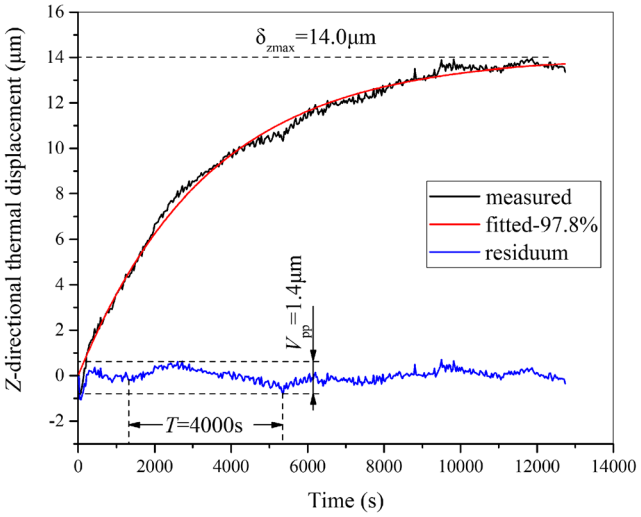

Fig. 11 Fitting effect of the thermal error model at 6000 rpm

The model above predicts that when the spindle speed increases, the change rate and maximum value of *Z*-directional thermal error decrease (as shown in Fig. 15). Furthermore, the change rate decreases with time. Therefore, the machining operation should be carried out at as high a spindle speed as possible and after preheating of the machine tool. The model predicts well and helps much in the machining process.

3.3.2 Y-directional thermal error prediction

According to Eqs. (26) and (27), the *Y*-directional thermal error prediction model is given as follows:

$$\delta_y = k(s)t + l(s), \tag{29}$$

where $k(s)$ is a function of s whose absolute value decreases with the increase of the spindle speed, $l(s)$ is a function of s whose absolute value increases with the increase of the spindle speed.

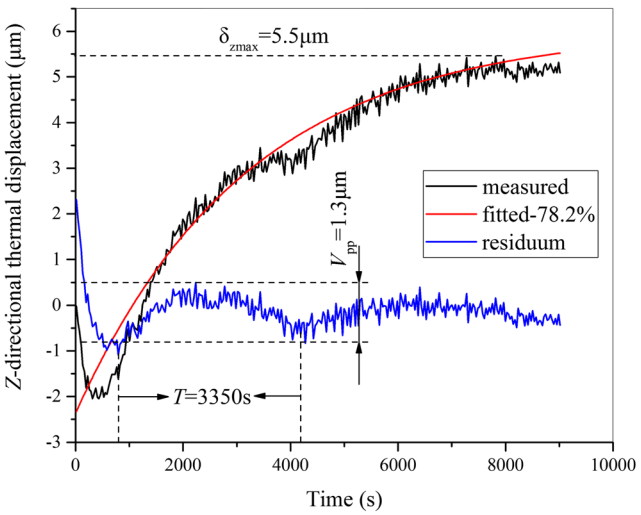

Fig. 12 Fitting effect of the thermal error model at 8000 rpm

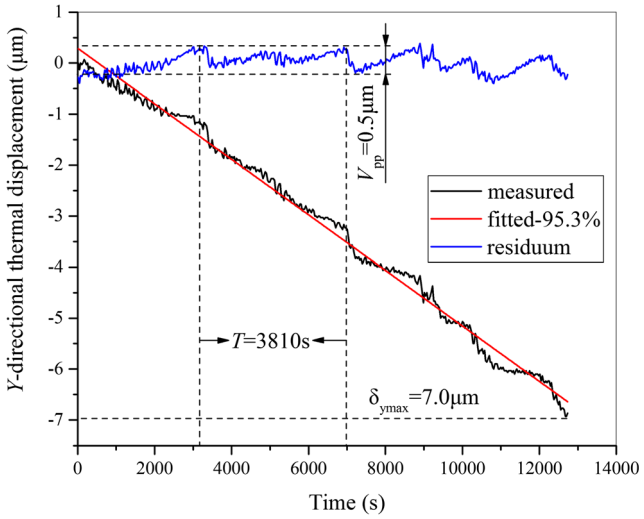

Fig. 13 Fitting effect of the thermal error model at 6000 rpm

The model above predicts that when the spindle speed increases, *Y*-directional thermal error changes acutely during the start-up process of the machine tool and more and more slowly after entering the stable operation stage (as shown in Fig. 16). The more dramatic changes in thermal error during the start-up process as the spindle speed increases are due to the increase of heat generation power and the operating delay of the cooling system. Therefore, the machining operation should be carried out at as high a spindle speed as possible and after preheating of the machine tool. The model predicts well and is very useful in improving machining precision.

3.4 Discussions

Thermal deformation is essentially a macroscopic behavior of thermoelastic distortion caused by the heat absorbed in the machine tool, considering from the point of view of heat instead of temperature, the complexity of thermal error

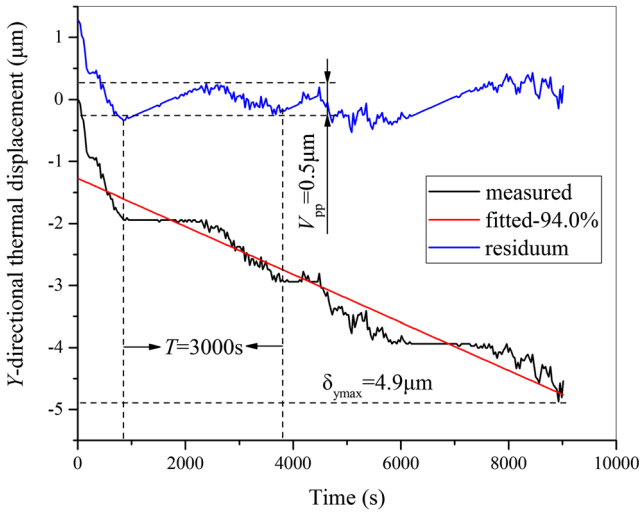

Fig. 14 Fitting effect of the thermal error model at 8000 rpm

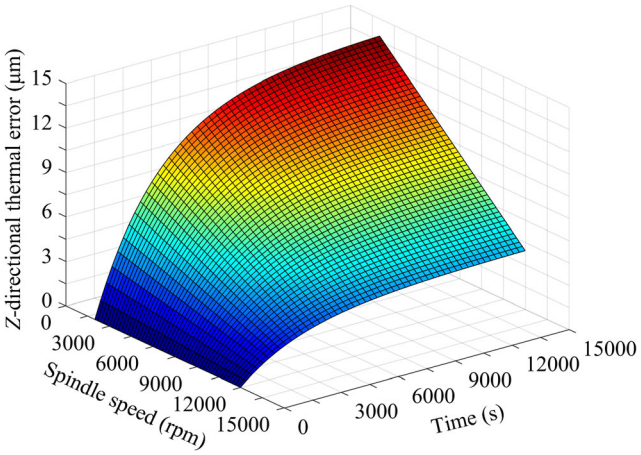

Fig. 15 *Z*-directional thermal error change at different spindle speeds

modeling can be greatly reduced. Actually, thermal deformations can be expressed as functions of heat quantity as known from the above analysis. Meanwhile, heat quantity is the function of heat-absorbing power and time, and thus, thermal deformation is the function of heat-absorbing power and time, too.

The functional relationships between the thermal deformations of parts of various shapes and heat quantity are different. And the thermal errors of a machine tool are closely related to its structure and the distribution of heat sources in it. Developing a system of thermal deformation models of typical machine tool parts will be very helpful to studying the thermal errors of the machine tool.

The proposed *Z*-directional and *Y*-directional thermal error models in this paper are of good accuracy and robustness, which verifies the effectiveness of the modeling method presented. Moreover, the models can easily be optimized by lessening the degree of structural simplification of the machine tool. Specifically, the quality of the *Z*-directional thermal error model is mainly affected by the simplification degree of the spindle structure. Further, the quality of the *Y*-directional

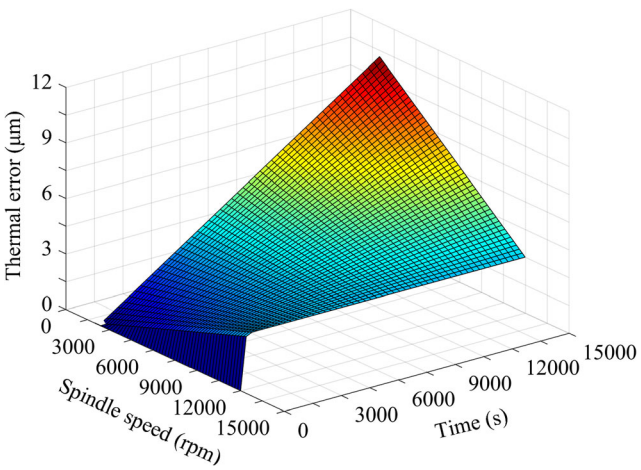

Fig. 16 *Y*-directional thermal error change at different spindle speeds

thermal error model is mainly affected by the simplification degree of the beam structure. Therefore, for instance, the *Z*-directional thermal error model can be optimized by lessening the simplification degree of the spindle structure. In addition, the models can be further optimized by further studying the distribution of heat sources in the machine tool and improving the calculation precision of heat quantity.

The proposed thermal error models can be used for thermal error prediction and provide suggestions for optimization of processing technology. The experimental results show that these models have a good prediction for thermal errors and are of high accuracy, which will contribute to the improvement of machining precision.

4 Conclusions

This paper presents a novel thermal error modeling method characterized by using heat quantity as the input variable. This method is established based on theoretical analysis of the essence of thermal deformation, with an emphasis on the analysis of heat source and machine structure. The derived theoretical formula used in the modeling process is verified correctness with FEA simulation, and the established models are also experimentally verified. The conclusions are as follows.

(1) The thermal error can be expressed as the function of heat quantity, which is still correct for general problems. The developed models with heat quantity as their input show good accuracy and robustness.

(2) The thermal deformation of a machine part is related to its shape and the locations of heat sources on it. And the thermal errors of a machine tool are closely related to its structure and the distribution of heat sources in it. It is an efficient method to study the thermal errors of a machine tool based on a system of thermal deformation models of typical machine tool parts and machine structures analysis.

(3) The proposed thermal error models are of good prediction capability and can be used for thermal error prediction and provide suggestions for optimization of processing technology.

(4) The relationships between the *Z*-directional thermal displacement of the TCP and e^{-t} and between the *Y*-directional thermal displacement of the TCP and time are approximately linear when the ambient temperature and the spindle speed are kept constant.

Study prospects This paper explored the essence of thermal deformation and deepened the research of thermal errors. Based on which, the newly proposed thermal error modeling method is more efficient and practical than the traditional way of using temperature as models' input. As the analysis of heat source and machine structure is essential for thermal error modeling using heat quantity, investigations about heat source and machine structure will be emphasized in future. Its aim is to improve the accuracy of thermal error models and implement thermal error compensation to meet the required machining precision and promote the application of relevant research results in the actual production.

Funding information This study received supports from the National Natural Science Foundation of China (grant No. 51575301), China Postdoctoral Science Foundation (grant No. 2017 M610880), and Shenzhen Foundational Research Project (Subject Layout) (grant No. JCYJ20160428181916222).

Nomenclature ΔH, Change in height (m); θ, Radian; β, Coefficient of volume expansion ($°C^{-1}$); q_1/q_2, Heat generation power of motor/bearing; γ, Grüneisen parameter ($Pa.m^3/J$) (W); K, Bulk modulus (Pa); n, Rotating speed (rpm); V, Volume (m^3); M, Total frictional torque (N.m); C_v, Heat capacity at constant volume (J/°C); T_σ, Average temperature of local area σ (°C); α, Linear expansion coefficient ($°C^{-1}$); q_{out}, Heat dissipation power to the air (W); ΔL, Change in length (m); K', Surface heat transfer coefficient; S, Area (m^2) ($W/(m^2.°C)$); t, Time (s); T_0, Ambient temperature (°C); c, Specific heat capacity (J/(kg.°C)); Q_{in}, Heat quantity absorbed (J); ρ, Density (kg/m^3); q_{all}, Total heat generation power (W); E, Heat quantity (J); q_{in}, Heat absorption power (W); E', Young's modulus (Pa); δ, Thermal displacement (m); μ, Poisson's ratio; T_S, Temperature of where near heat source; λ, Thermal Conductivity (W/(m.°C)) (°C); ΔT, Change in temperature (°C)

References

1. Bryan J (1990) International status of thermal error research (1990). CIRP Ann 39(2):645–656. https://doi.org/10.1016/S0007-8506(07)63001-7
2. Qianjian G, Jianguo Y (2011) Application of projection pursuit regression to thermal error modeling of a CNC machine tool. Int J Adv Manuf Technol 55(5):623–629. https://doi.org/10.1007/s00170-010-3114-4
3. Tan F, Yin M, Wang L, Yin G (2018) Spindle thermal error robust modeling using LASSO and LS-SVM. Int J Adv Manuf Technol 94(5):2861–2874. https://doi.org/10.1007/s00170-017-1096-1
4. Ramesh R, Mannan MA, Poo AN (2000) Error compensation in machine tools—a review: part II: thermal errors. Int J Mach Tools Manuf 40(9):1257–1284. https://doi.org/10.1016/S0890-6955(00)00010-9
5. Vyroubal J (2012) Compensation of machine tool thermal deformation in spindle axis direction based on decomposition method. Precis Eng 36(1):121–127. https://doi.org/10.1016/j.precisioneng.2011.07.013
6. Li Y, Zhao W, Wu W, Lu B (2017) Boundary conditions optimization of spindle thermal error analysis and thermal key points selection based on inverse heat conduction. Int J Adv Manuf Technol 90(9):2803–2812. https://doi.org/10.1007/s00170-016-9594-0
7. Bossmanns B, Tu JF (1999) A thermal model for high speed motorized spindles. Int J Mach Tools Manuf 39(9):1345–1366. https://doi.org/10.1016/S0890-6955(99)00005-X
8. Liu Z, Pan M, Zhang A, Zhao Y, Yang Y, Ma C (2014) Thermal characteristic analysis of high-speed motorized spindle system based on thermal contact resistance and thermal-conduction resistance. Int J Adv Manuf Technol 76(9–12):1913–1926. https://doi.org/10.1007/s00170-014-6350-1

9. Li Y, Zhao W, Lan S, Ni J, Wu W, Lu B (2015) A review on spindle thermal error compensation in machine tools. Int J Mach Tools Manuf 95:20–38. https://doi.org/10.1016/j.ijmachtools.2015.04.008
10. Li Y, Zhao W, Wu W, Lu B, Chen Y (2014) Thermal error modeling of the spindle based on multiple variables for the precision machine tool. Int J Adv Manuf Technol 72(9–12):1415–1427. https://doi.org/10.1007/s00170-014-5744-4
11. Yan K, Hong J, Zhang J, Mi W, Wu W (2016) Thermal-deformation coupling in thermal network for transient analysis of spindle-bearing system. Int J Therm Sci 104:1–12. https://doi.org/10.1016/j.ijthermalsci.2015.12.007
12. Li X, Lv Y, Yan K, Liu J, Hong J (2017) Study on the influence of thermal characteristics of rolling bearings and spindle resulted in condition of improper assembly. Appl Therm Eng 114:221–233. https://doi.org/10.1016/j.applthermaleng.2016.11.194
13. Cao H, Zhang X, Chen X (2016) The concept and progress of intelligent spindles: a review. Int J Mach Tools Manu 112:21–52. https://doi.org/10.1016/j.ijmachtools.2016.10.005
14. Chen J-S, Hsu W-Y (2003) Characterizations and models for the thermal growth of a motorized high speed spindle. Int J Mach Tools Manuf 43(11):1163–1170. https://doi.org/10.1016/S0890-6955(03)00103-2
15. Uhlmann E, Hu J (2012) Thermal modelling of a high speed motor spindle. Procedia CIRP 1(Supplement C):313–318. https://doi.org/10.1016/j.procir.2012.04.056
16. Yang J, Shi H, Feng B, Zhao L, Ma C, Mei X (2015) Thermal error modeling and compensation for a high-speed motorized spindle. Int J Adv Manuf Technol 77(5):1005–1017. https://doi.org/10.1007/s00170-014-6535-7
17. Shi H, Ma C, Yang J, Zhao L, Mei X, Gong G (2015) Investigation into effect of thermal expansion on thermally induced error of ball screw feed drive system of precision machine tools. Int J Mach Tools Manuf 97:60–71. https://doi.org/10.1016/j.ijmachtools.2015.07.003
18. Zhang C, Gao F, Yan L (2017) Thermal error characteristic analysis and modeling for machine tools due to time-varying environmental temperature. Precis Eng 47(Supplement C):231–238. https://doi.org/10.1016/j.precisioneng.2016.08.008
19. Chow JH, Zhong ZW, Lin W, Khoo LP, Kiew CM (2015) A finite-difference thermal model of a three-phase coreless linear motor as a heat source. Appl Therm Eng 87(Supplement C):605–614. https://doi.org/10.1016/j.applthermaleng.2015.05.064
20. Liu Q, Yan J, Pham DT, Zhou Z, Xu W, Wei Q, Ji C (2016) Identification and optimal selection of temperature-sensitive measuring points of thermal error compensation on a heavy-duty machine tool. Int J Adv Manuf Technol 85(1):345–353. https://doi.org/10.1007/s00170-015-7889-1
21. Wang L, Wang H, Li T, Li F (2015) A hybrid thermal error modeling method of heavy machine tools in z-axis. Int J Adv Manuf Technol 80(1–4):389–400. https://doi.org/10.1007/s00170-015-6988-3
22. Yang H, Ni J (2005) Dynamic neural network modeling for nonlinear, nonstationary machine tool thermally induced error. Int J Mach Tools Manuf 45(4–5):455–465. https://doi.org/10.1016/j.ijmachtools.2004.09.004
23. Brecher C, Hirsch P, Weck M (2004) Compensation of thermo-elastic machine tool deformation based on control internal data. CIRP Ann 53(1):299–304. https://doi.org/10.1016/S0007-8506(07)60702-1
24. Jin C, Wu B, Hu Y, Yi P, Cheng Y (2015) Thermal characteristics of a CNC feed system under varying operating conditions. Precis Eng 42(Supplement C):151–164. https://doi.org/10.1016/j.precisioneng.2015.04.010
25. Mokdad F, Chen DL, Liu ZY, Ni DR, Xiao BL, Ma ZY (2017) Hot deformation and activation energy of a CNT-reinforced aluminum matrix nanocomposite. Mater Sci Eng A 695:322–331. https://doi.org/10.1016/j.msea.2017.04.006
26. Galant A, Beitelschmidt M, Großmann K (2016) Fast high-resolution FE-based simulation of thermo-elastic behaviour of machine tool structures. Procedia CIRP 46:627–630. https://doi.org/10.1016/j.procir.2016.04.020
27. Liu ZJ, Song T, Sun XW, Ma Q, Wang T, Guo Y (2017) Thermal expansion, heat capacity and Grüneisen parameter of iridium phosphide Ir2P from quasi-harmonic Debye model. Solid State Commun 253:19–23. https://doi.org/10.1016/j.ssc.2017.01.028
28. Haitao Z, Jianguo Y, Jinhua S (2007) Simulation of thermal behavior of a CNC machine tool spindle. Int J Mach Tools Manuf 47(6):1003–1010. https://doi.org/10.1016/j.ijmachtools.2006.06.018